Vol. 4, No. 2, 2023

Vitaliy Korendiy, Oleksandr Kachur, Mykola Boikiv, Yurii Novitskyi, Oleksandr Yaniv
Lviv Polytechnic National University
12, S. Bandery Str., Lviv, 79013, Ukraine

https://doi.org/10.23939/tt2023.02.056

ANALYSIS OF KINEMATIC CHARACTERISTICS OF A MOBILE CATERPILLAR ROBOT WITH A SCARA-TYPE MANIPULATOR

Summary. *Automation and robotization of various production and technological processes in many industries is one of the leading trends in the development of modern society. Industrial robots have recently become quite widespread, and it is almost impossible to imagine any modern production in the fields of mechanical engineering (machine building), instrumentation, pharmaceuticals, food, chemical industries, etc., without robotic complexes. Over the past few decades, another area of robotics has emerged: autonomous mobile robots. It combines research in mechanics, electronics, and computer technologies, including artificial intelligence.*

Among the most common applications of autonomous mobile robots are the performance of various technological operations in places that are dangerous to human life (radiation, biological or chemical contamination) or uninhabitable (space, sea depths, volcanic craters, etc.). Mobile robots have also proven themselves in rescue operations during cataclysms and natural disasters, anti-terrorist operations, military operations, mine clearance, etc.

Given the urgency of the issue of mobile robotics development, this article proposes a new design of an autonomous robotic complex built on the basis of a tracked chassis and equipped with a SCARA-type manipulator. The main task of the developed robot is to perform various technological operations in places where human presence is dangerous or impossible, in particular, when performing demining tasks. In the course of the research, the kinematics of the manipulator was analyzed in detail to determine its working area, and the kinematic parameters of the tracked chassis were experimentally tested while it was moving over rough terrain. The obtained results can be used to further improve the design and control system of the robot and manipulator and in the process of determining the specific technological tasks that will be assigned to this robotic platform.

Keywords: *mobile robot, robotic complex, tracked chassis, territory demining, manipulator kinematics, manipulator working area, motion over rough terrain.*

1. INTRODUCTION

Modern mobile robots have a significant export potential that can compensate for the costs of their development and generate profits from foreign supplies [1]. Therefore, in many developed countries, firms with advanced information and production technologies are striving to create samples of competitive mobile robots for various purposes [2, 3]. Among a great variety of mobile robots, the tracked (caterpillar) and wheeled ones are the most widespread [4, 5]. The following models can be considered among the most advanced in their classes: 1) SWORDS MAARS (Fig. 1, *a*) by Foster-Miller (USA) – designed for reconnaissance, destruction of manpower and equipment, detection and neutralization of explosive devices [6]; 2) ANDROS Mark (Fig. 1, *b*) by Remotec (USA) – designed for reconnaissance and technological operations at industrial and nuclear facilities, impact on control panel elements (buttons, switches, regulators) and pipelines (valves, valves, etc.) [7]; 3) Centaur (Fig. 1, *c*) by FLIR Systems (USA) – designed for detecting, confirming, identifying and disposing of various hazards including unexploded

ordnance, landmines, and improvised explosive devices [8]; 4) TEODor (Fig. 1, *d*) by Telerob Gesellschaft fur Fernhantierungstechnik mbH (Germany) – designed to detect and neutralize explosive devices, eliminate the consequences of emergencies, and anti-terrorist operations [9]; Telemax EVO (Pro, Plus, Hybrid) (Fig. 1, *e*) by AeroVironment (USA) – designed to disarm improvised explosive devices and investigate chemical, biological, radiological and nuclear hazards [10]; Husky (Grizzly) by Clearpath Robotics (USA) – designed for challenging outdoor usage, grasping objects, closing valves, etc. [11].

a *b* *c* *d* *e* *f*

Fig. 1. Recent designs of mobile robots for different purposes

Numerous scientific papers are dedicated to various aspects of designing, manufacturing, maintenance, experimental testing, and practical implementation of mobile robots [1–6]. An interesting and prospective direction of development of such robotic systems is pipeline inspection using vibration-driven locomotion systems [12, 13]. Nevertheless, the leading trends in current robotics are focused on tracked (caterpillar) and wheeled robots [14–25]. The novel control and maneuverability approaches of mobile tracked robots are studied thoroughly in [14, 15]. The papers [16, 17] are devoted to the enhanced design peculiarities of autonomous articulated robots. In [18–21], the authors investigated various obstacle-avoidance and navigation systems of tracked robots. The research on path-planning and locomotion system performance of mobile robotic systems are considered in [22, 23]. The investigations on the dynamic behavior and suspension operation of caterpillar robots are carried out in [24, 25]. Numerous other publications deal with different aspects of implementing mobile robotic systems, and the present research is focused on the enhanced design of a tracked platform developed at Lviv Polytechnic National University and equipped with a SCARA-type manipulator. The major objectives of this research consist in analyzing design peculiarities and kinematic characteristics of the proposed robot and manipulator intended for performing various military operations, particularly the detection and neutralization of explosive devices.

2. RESEARCH PURPOSE STATEMENT

The purpose of the present research is to comprehensively analyze the design peculiarities and kinematic characteristics of an enhanced tracked (caterpillar) robot equipped with a SCARA-type manipulator. The following tasks are accomplished to reach this goal:

- to analyze the design peculiarities of an enhanced tracked (caterpillar) robot;
- to consider the structure and design of the developed SCARA-type manipulator;
- to carry out mathematical modeling and computer simulation of the manipulator motion;
- to conduct experimental tests on the robot`s motion along a rugged terrain.

3. GENERAL DESIGN OF THE ENHANCED ROBOTIC PLATFORM

The novel design of the mobile robotic complex has been developed at Lviv Polytechnic National University and is presented in Fig. 2. The solid-state model of the robot is designed in the SolidWorks software and consists of three main units: tracked platform 1, electronic control unit 2, manipulator 3.

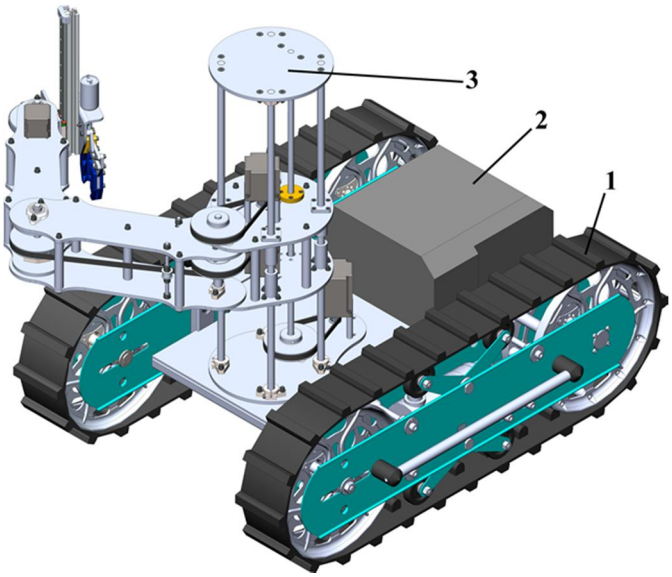

Fig. 2. General design of the caterpillar robot with the SCARA-type manipulator

The robot is designed to perform various technological operations on a rugged terrain, particularly to detect and neutralize explosive devices. The tracked platform is used to carry the manipulator and to

conduct its general orientation. The platform (see Fig. 3) consists of the installation plate 1, on which the manipulator and electronic control unit 3 are fixed. The rubber (or polyurethane) dampers 4 are used to suspend the plate 1 from the caterpillar units 2. The front wheels 6 are non-driven, and their axles can change their positions while regulating the tension of the tracks (caterpillars) 9. The rear wheels 7 are set into motion by the electric geared motors 5 using the chain transmission, which consists of the driving sprocket 10, driven sprocket 12, and chain 11. Each motor is characterized by the consumed power of 100 W, voltage of 24 V, gear ratio of 20, and nominal output rotation frequency of 150 rpm. The chain transmission ratio is 1.5. To stabilize the position and tension of the tracks 9 when the robot overcomes different obstacles, the additional V-shaped lever mechanisms 8 are used. All the components of the caterpillar units are installed between two rigidly fixed plates 2. The proposed design of the tracked platform can move on rough terrain with a maximal speed of approximately 8…10 km/h and can overcome obstacles with a maximal height of about 30 cm. The nominal duration of the autonomous operation of the robot depends on the batteries used and the working modes. In general, it is planned that the robot should be able to perform its technological operations for at least 2 hours.

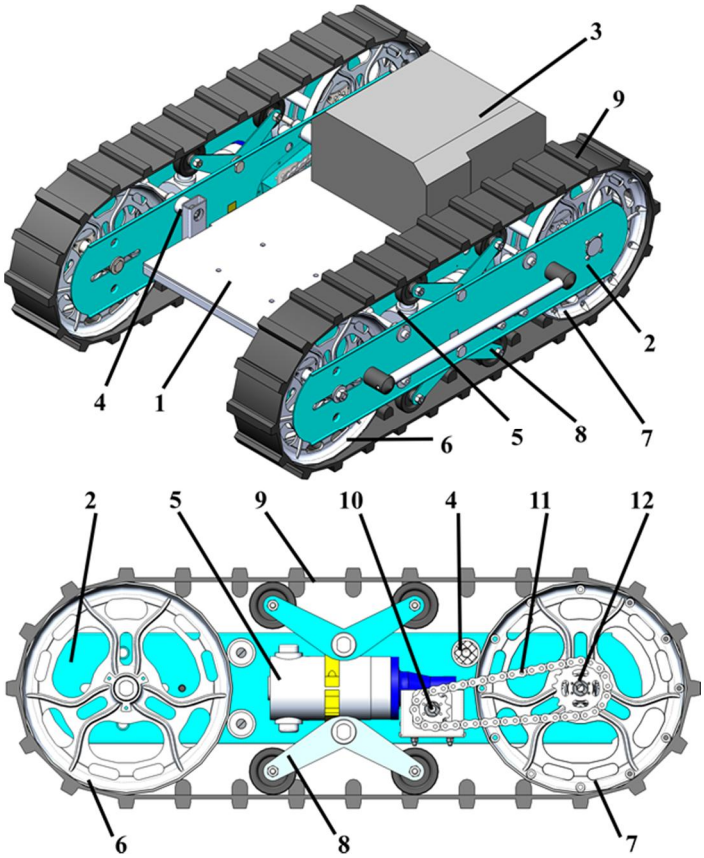

Fig. 3. Tracked platform of the mobile robot

The general design of the mobile robot's manipulator intended to hold and carry cylindrical parts of about 1 kg mass is shown in Fig. 4. The manipulator is mounted on the robot's platform using plate 1, on which the electric motor 2 of the vertical movement drive and the corresponding guides 3 are installed. The torque is transmitted from the shaft of the electric motor 2 to the drive screw 4 of the vertical movement mechanism of the manipulator using the toothed belt transmission 5. Platform 6 of vertical movement, on which nut 7 of the screw-nut transmission is fixed, has the ability to slide along guides 3 due to the rotation of screw 4. The electric motor 8 for driving the rotational movement of the first link 9 of the manipulator is installed on platform 6. As in the previous case, the torque from the shaft of the electric motor 8 to the drive shaft of the first rotating link 9 of the manipulator is transmitted through the toothed belt drive 10. An

electric motor 11 of the drive of the rotational movement of the second link 12 of the manipulator is installed on platform 6. The shaft of the electric motor 11 and the rotary shaft of the link 12 are connected by two toothed belt transmissions 13. The electric motor 14 of the rotational movement of the gripper 15 is installed on the link 12. The torque is transmitted from the shaft of the electric motor 14 to the corresponding shaft of the bracket 16 of the gripper 15 using a gear (toothed) quadrant 17. The gripper 15 is mounted on a rotary bracket 16 with the possibility of adjusting its vertical position by sliding along a profile guide, which is provided by a toothed belt drive 18. The drive pulley of the belt drive 18 is fixed on the shaft of the electric motor 19.

The manipulator operates as follows. If it is necessary to change the vertical position of the gripper within insignificant limits (100–150 mm), the vertical movement drive (electric motor 19 and tooth-belt transmission 18) is used to move the gripper along the guide attached to the bracket 16. Larger vertical movements of the gripper are carried out by raising/lowering the manipulator platform 6, which occurs when the motor 2 is activated, and the screw 4 of the screw-nut transmission is rotated through the toothed belt transmission 5. The movement of the gripper in the horizontal plane is carried out by two drives of rotational movement of the first 9 and the second 12 links of the manipulator, as well as by the drive of rotation of the gripper 15 through the gear quadrant 17. The latter is used exclusively for high-precision positioning of the gripper relative to the surfaces of the parts that must interact with the gripping jaws.

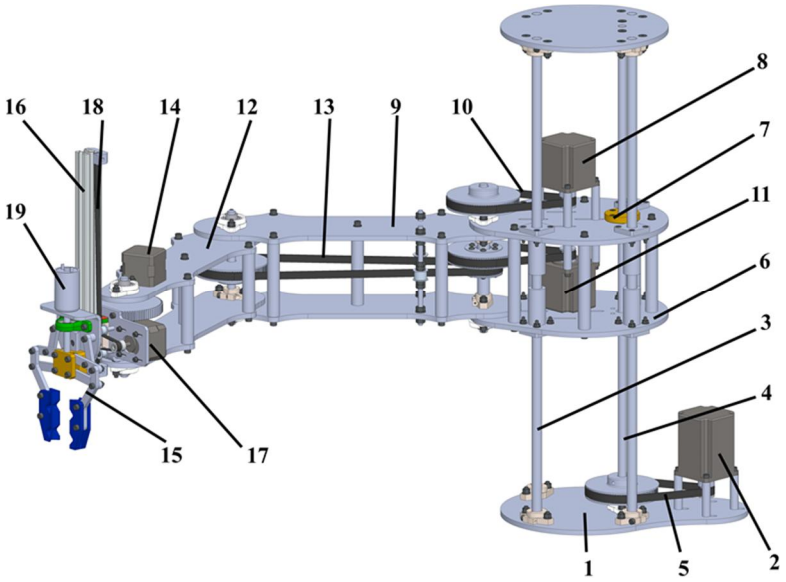

Fig. 4. General design of the SCARA-type manipulator

4. KINEMATIC ANALYSIS OF THE SCARA-TYPE MANIPULATOR

Following the developed general design of the manipulator (Fig. 4), the simplified kinematic diagram of its mechanical system is shown in Fig. 5. The prismatic slider *A* provides the vertical translational movement of the platform 6 of the manipulator; the cylindrical joint *B* provides rotation of the first link 9 of the manipulator relative to the platform 6; the cylindrical joint *C* is responsible for the rotation of the second link 12 of the manipulator relative to the first link 9; the cylindrical joint *D* provides rotation of the gripper bracket 16 relative to the second link 12 of the manipulator; the prismatic slider *E* is used to move the gripper 15 in vertical direction. To calculate the degree of mobility of the manipulator (the number of degrees of freedom), we use the following formula for spatial mechanisms:

$$W = 6 \cdot n - 5 \cdot p_5 - 4 \cdot p_4 - 3 \cdot p_3 - 2 \cdot p_2 - p_1, \tag{1}$$

where n is the number of movable links of the manipulator; p_5 is the number of the kinematic pairs of the fifth class (single-move pairs); p_i is the number of the kinematic pairs of the i-th class ($i = 1, 2, 3, 4, 5$).

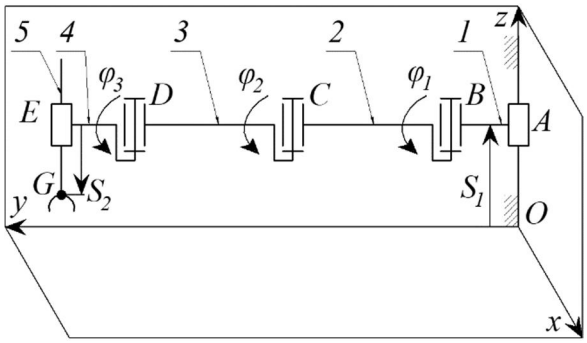

Fig. 5. Simplified kinematic diagram of the SCARA-type manipulator

In accordance with the kinematic diagram of the manipulator (Fig. 5), the mechanism has 5 movable links ($n = 5$) and 5 kinematic pairs of the fifth class (single-move pairs) ($p_5 = 5$): two translational pairs (prismatic sliders *A* and *E*) and three rotational (revolute) pairs (cylindrical joints *B*, *C*, *D*). There are no higher kinematic pairs in the mechanism, thus $p_1 = p_2 = p_3 = p_4 = 0$. Therefore, considering Eq. (1), the degree of mobility of the manipulator (the number of degrees of freedom) is equal to:

$$W = 6 \cdot 5 - 5 \cdot 5 - 4 \cdot 0 - 3 \cdot 0 - 2 \cdot 0 - 0 = 5.$$

Based on the carried-out calculation, we can state that it is enough to know the laws of change of five generalized coordinates to unambiguously determine the position of the gripper (point *G*) in space at a certain point in time. Let us choose an inertial reference system (spatial Cartesian coordinate system) centered at the point *O*, which is located on the screw axis of the mechanism of vertical movement of the manipulator (see Figs. 4 and 5). In this case, we assume that the horizontal plane *xOy* coincides with the fixed platform attached to the robot chassis. Let us accept the following generalized coordinates:

S_1 – vertical displacement of the slider *A* relative to the fixed platform (the *xOy* plane); the positive value of the coordinate S_1 coincides with the direction of the *Oz* axis (see Fig. 5);

φ_1 – the angle of rotation of the first link of the manipulator (rod *BC*) relative to the platform (the positive value of the angle is plotted in an anticlockwise direction relative to the plane *zOy*, which is parallel to the longitudinal axis of the robot chassis (the axis coincides with the direction of the robot's straight-line movement, see Fig. 6);

φ_2 – the angle of rotation of the second link of the manipulator (rod *CD*) relative to the first link (rod *BC*) (the initial position of the links assumes their parallelism with a positive angle value being set in an anticlockwise direction, see Fig. 6);

φ_3 – angle of rotation of the gripper mounting bracket (rod *DE*) relative to the second link of the manipulator (rod *CD*) (the initial position of the links implies their parallelism with a positive angle value being set in anticlockwise direction, see Fig. 6);

S_2 – vertical displacement of the slider guide *E* relative to the movable platform of the manipulator (a plane parallel to the horizontal plane *xOy* and passing through the rods *BC*, *CD*, *DE*); the positive value of the coordinate S_2 is opposite to the direction of the *Oz* axis (see Fig. 5).

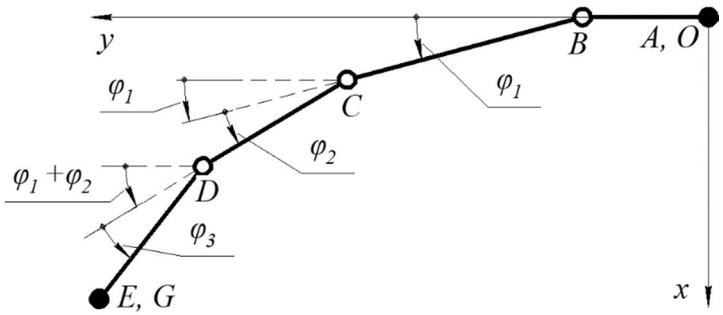

Fig. 6. The diagram illustrating the generalized coordinates related with the revolute kinematic pairs of the manipulator

Let us derive the laws of motion of the corresponding kinematic pairs of the manipulator mechanism in the form of functional dependencies on the adopted generalized coordinates:

– slider *A* (see Fig. 5):

$$x_A = 0, \quad y_A = 0, \quad z_A = S_1; \tag{2}$$

– cylindrical joint *B* (see Figs. 5 and 6):

$$x_B = x_A = 0, \quad y_B = y_A + l_{AB} = l_{AB}, \quad z_B = z_A = S_1; \tag{3}$$

– cylindrical joint *C* (see Figs. 5 and 6):

$$x_C = x_B + l_{BC} \cdot \sin\varphi_1 = l_{BC} \cdot \sin\varphi_1, \quad y_C = y_B + l_{BC} \cdot \cos\varphi_1 = l_{AB} + l_{BC} \cdot \cos\varphi_1, \quad z_C = z_B = S_1; \tag{4}$$

– cylindrical joint *D* (see Figs. 5 and 6):

$$\begin{gathered} x_D = x_C + l_{CD} \cdot \sin(\varphi_1 + \varphi_2) = l_{BC} \cdot \sin\varphi_1 + l_{CD} \cdot \sin(\varphi_1 + \varphi_2), \\ y_D = y_C + l_{CD} \cdot \cos(\varphi_1 + \varphi_2) = l_{AB} + l_{BC} \cdot \cos\varphi_1 + l_{CD} \cdot \cos(\varphi_1 + \varphi_2), \qquad z_D = z_C = S_1; \end{gathered} \tag{5}$$

– slider *E* (see Figs. 5 and 6):

$$\begin{gathered} x_E = x_D + l_{DE} \cdot \sin(\varphi_1 + \varphi_2 + \varphi_3) = l_{BC} \cdot \sin\varphi_1 + l_{CD} \cdot \sin(\varphi_1 + \varphi_2) + l_{DE} \cdot \sin(\varphi_1 + \varphi_2 + \varphi_3), \\ y_E = y_D + l_{DE} \cdot \cos(\varphi_1 + \varphi_2 + \varphi_3) = l_{AB} + l_{BC} \cdot \cos\varphi_1 + l_{CD} \cdot \cos(\varphi_1 + \varphi_2) + l_{DE} \cdot \cos(\varphi_1 + \varphi_2 + \varphi_3), \\ z_E = z_D = S_1; \end{gathered} \tag{6}$$

– gripper (point *G*, see Fig. 5):

$$\begin{gathered} x_G = x_E = l_{BC} \cdot \sin\varphi_1 + l_{CD} \cdot \sin(\varphi_1 + \varphi_2) + l_{DE} \cdot \sin(\varphi_1 + \varphi_2 + \varphi_3), \\ y_G = y_E = l_{AB} + l_{BC} \cdot \cos\varphi_1 + l_{CD} \cdot \cos(\varphi_1 + \varphi_2) + l_{DE} \cdot \cos(\varphi_1 + \varphi_2 + \varphi_3), \\ z_G = z_E - S_2 = S_1 - S_2, \end{gathered} \tag{7}$$

where l_{AB}, l_{BC}, l_{CD}, l_{DE} are the lengths of the corresponding links of the manipulator mechanism.

Based on the solid-state model of the manipulator developed in the SolidWorks software, we simulated the movement of the gripper, based on the results of which we built a corresponding trajectory (Fig. 7) characterizing the working area of the manipulator.

Using the derived equations (7) of motion of the gripper of the manipulator, it is possible to plot the trajectories of its movement and determine the speeds and accelerations at any point of the trajectory under the known laws of change of the generalized coordinates. In order to carry out numerical modeling of the manipulator's motion using the derived equations of motion of the gripper in the MathCad software, it is necessary to set the geometric parameters of the manipulator and the laws of change of the corresponding generalized coordinates. In accordance with the above-mentioned notations and the solid model of the manipulator (Figs. 4 and 7), we have: $l_{AB} = 120$ mm, $l_{BC} = 300$ mm, $l_{CD} = 300$ mm, $l_{DE} = 87$ mm. To determine the time dependencies of the generalized coordinates of the manipulator, we divide the time interval of its movement into several intervals. In accordance with the trajectory of the gripper shown in Fig. 7, the laws of change of the corresponding generalized coordinates are as follows:

– at the first stage ($t = 0...2$ s):

$$\varphi_1(t) = -60° = const, \quad \varphi_2(t) = -75° = const, \quad \varphi_3(t) = -76° + 38° \cdot t \neq const;$$

– at the second stage ($t = 2...4$ s):

$$\varphi_1(t) = -60° = const, \quad \varphi_2(t) = -75° + 37{,}5° \cdot (t-2) \neq const, \quad \varphi_3(t) = 0° = const;$$

– at the third stage ($t = 4...6$ s):

$$\varphi_1(t) = -60° + 60° \cdot (t-4) \neq const, \quad \varphi_2(t) = 0° = const, \quad \varphi_3(t) = 0° = const;$$

– at the fourth stage ($t = 6...8$ s):

$$\varphi_1(t) = 60° = const, \quad \varphi_2(t) = 37{,}5° \cdot (t-6) \neq const, \quad \varphi_3(t) = 0° = const;$$

– at the fifth stage ($t = 8...10$ s):

$$\varphi_1(t) = 60° = const, \quad \varphi_2(t) = 75° = const, \quad \varphi_3(t) = 38° \cdot (t-8) \neq const;$$

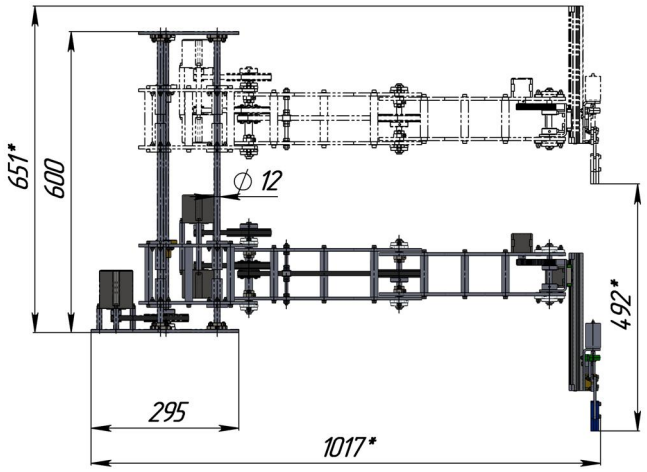

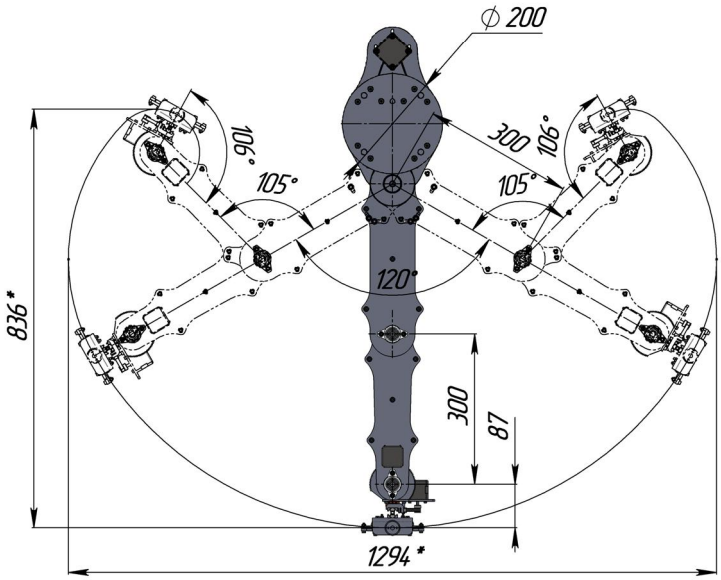

Fig. 7. The geometric parameters of the links and the working area of the manipulator, obtained as a result of simulation of its movement in the SolidWorks software

Substituting the geometric parameters of the manipulator into the equations (7) of motion of the gripper and setting the laws of change of the generalized coordinates for the corresponding time intervals, the corresponding trajectory of the gripper, which determines the working area of the manipulator, is plotted in the MathCad software (Fig. 8). The maximum displacement of the gripper along the *Oy* axis is approximately 840 mm (at the limit positions of + 30 mm and –

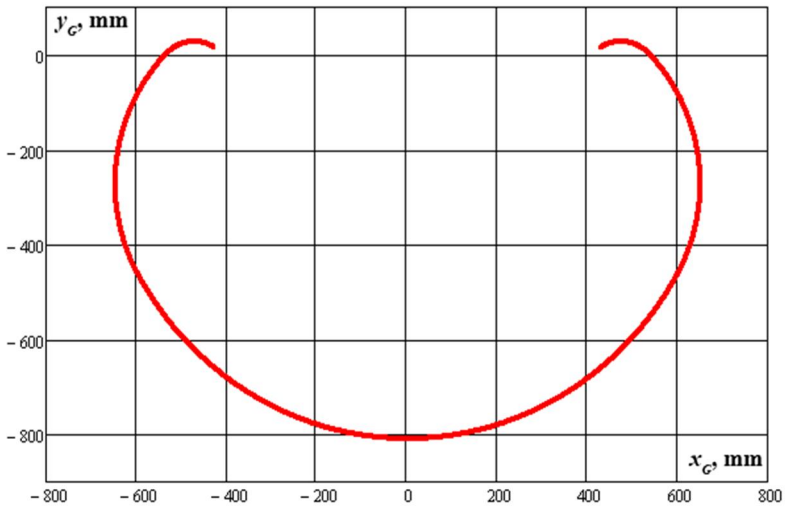

Fig. 8. Trajectory of the gripper motion modeled in the MathCad software

810 mm); the maximum displacement of the gripper along the *Ox* axis is about 1300 mm (at the limit positions of + 650 mm and – 650 mm). The obtained values are in full agreement with the results of the simulation conducted in the SolidWorks software: according to the data shown in Fig. 7, the maximum displacement of the gripper along the *Oy* axis is 836 mm, and along the *Ox* axis – 1294 mm. The highest vertical position of the gripper is about + 300 mm above the manipulator's fixation plate, and the lowest position is approximately – 200 mm.

Taking into account the results of numerical modeling in the MathCad software (Fig. 8) and computer simulation in the SolidWorks software (Fig. 7), it can be concluded that the derived analytical dependencies (1)–(7) adequately describe the gripper's motion conditions and can be used while developing and programming the corresponding control system of the proposed SCARA-type manipulator.

5. EXPERIMENTAL STUDIES ON THE ROBOT MOTION CONDITIONS

The full-scale laboratory prototype of the mobile tracked (caterpillar) robot (see Fig. 9) was manufactured at Lviv Polytechnic National University. The experimental investigations were carried out during the robot motion at a horizontal speed of about 8 km/h along a rugged terrain. The WitMotion sensor BWT901CL was used to measure the vertical accelerations of the robot's body at the place of fixation of the SCARA-type manipulator. The sensor allows for detecting the vibrations at the bandwidth of 256 Hz, baud rate of 92160 bauds, output rate of 200 Hz, and acceleration range of ±16g (±157 m/s^2). The information from the sensor is sent with the help of the Bluetooth interface to the laptop with the corresponding WitMotion software installed (see Fig. 9). The MathCad software is used to transform the tabular data received from the WitMotion software into the graphical (plotted) dependencies.

The obtained experimental data is presented by the time dependency of the robot's body vertical acceleration during its motion along a rough terrain (see Fig. 10). The measured accelerations can be used to determine the inertial loads acting upon the links and gripper of the manipulator. The mentioned loads influence the gripping forces needed to be provided to effectively hold and carry the cylindrical parts (or workpieces) of the 1 kg mass (10 N weight). The maximal value of the robot's body vertical acceleration reaches 1 g (9.81 m/s^2) in the upward direction and 0.85 g (8.34 m/s^2) in the downward. Therefore, the maximal vertical overloading of the gripper holding the part (piecewise) can reach 2. It allows for concluding, that while performing calculations of the gripper, it is necessary to consider the maximal weight of the part to be carried by the manipulator of approximately 20 N (2 kgF).

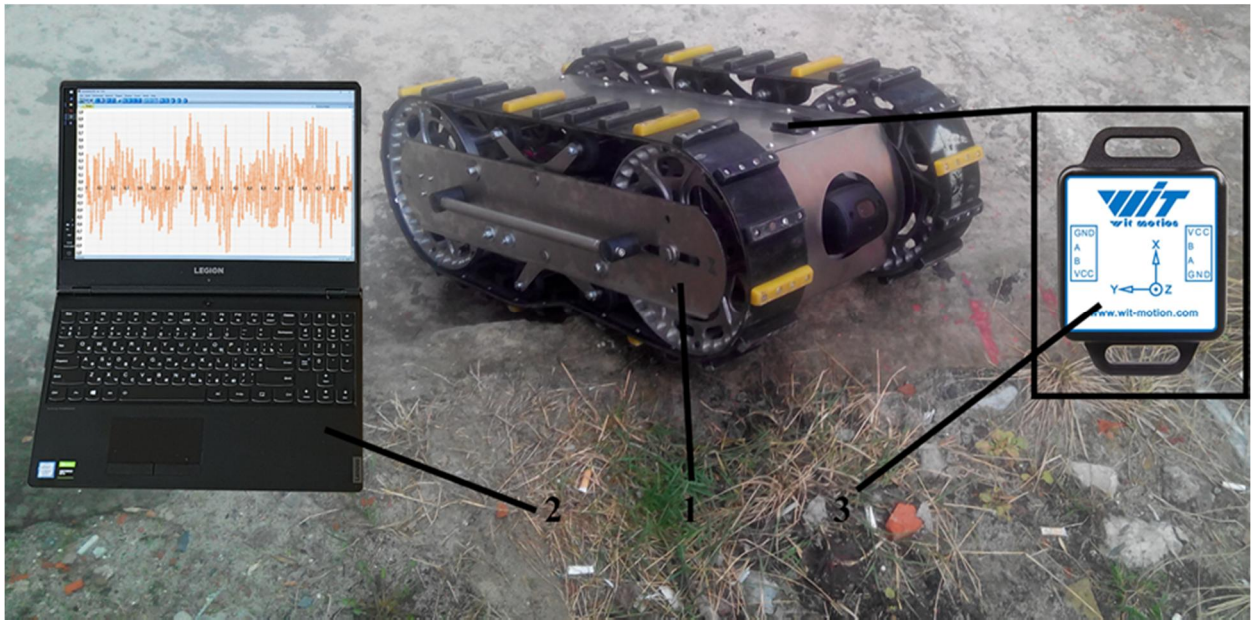

Fig. 9. Experimental equipment used for analyzing the robot's kinematic characteristics

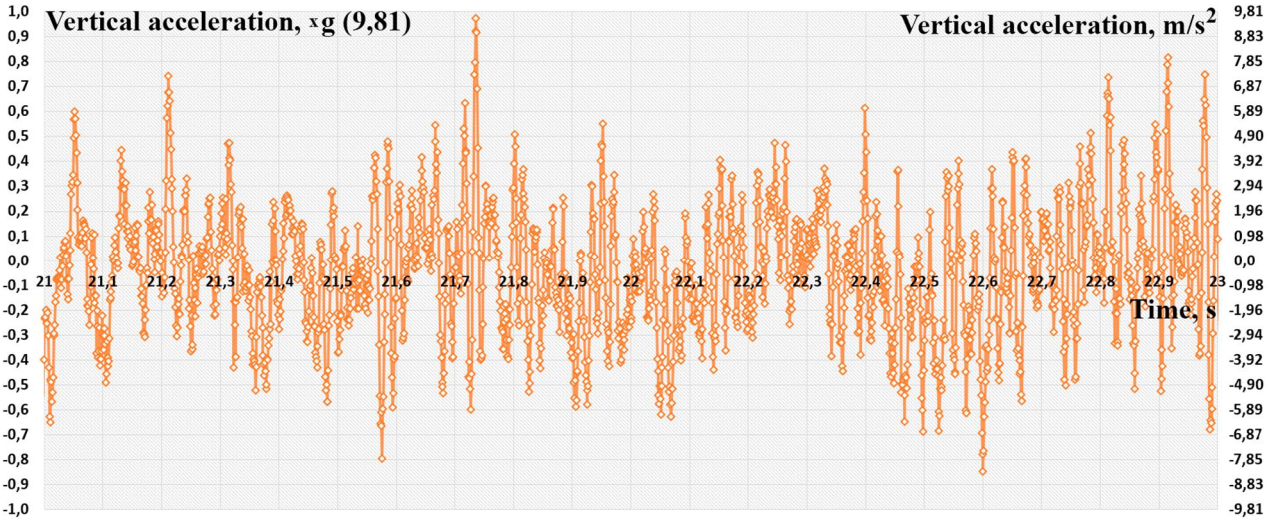

Fig. 10. Vertical accelerations of the robot's body during its motion along a rugged terrain

6. CONCLUSIONS

The paper considers the enhanced design of the mobile tracked (caterpillar) robot equipped with the SCARA-type manipulator. The robot can reach a motion speed of about 8…10 m/s and is driven by two electric motors of 100 W power each. The SCARA-type manipulator is designed to hold and carry the cylindrical parts (workpieces) of the mass up to 1 kg. Based on the performed kinematic analysis of the manipulator, the corresponding working zone of the gripper is analytically described and simulated. The maximum displacement of the gripper along the Oy axis is approximately 840 mm (at the limit positions of + 30 mm and – 810 mm); the maximum displacement of the gripper along the Ox axis is about 1300 mm (at the limit positions of + 650 mm and – 650 mm). The experimental investigations are carried out during the robot motion at a horizontal speed of about 8 km/h along a rugged terrain. The obtained experimental data is presented by the time dependency of the robot's body vertical acceleration. The maximal value of the acceleration reaches 1 g (9.81 m/s2) in the upward direction and 0.85 g (8.34 m/s2) in the downward. The obtained results can be used by researchers and designers of similar robotic systems while calculating the caterpillar drives, manipulators, and gripping devices. Further investigations on the subject of the paper can be focused on the mathematical modeling and computer simulation of the robot's suspension dynamic behavior and investigating the force-power characteristics of the transmission.

References

1. Dong, L., He, Z., Song, C., & Sun, C. (2023). A review of mobile robot motion planning methods: from classical motion planning workflows to reinforcement learning-based architectures. *Journal of Systems Engineering and Electronics*, *34*(2), 439–459. doi: 10.23919/JSEE.2023.000051 (in English).

2. Mikołajczyk, T., Mikołajewski, D., Kłodowski, A., Łukaszewicz, A., Mikołajewska, E., Paczkowski, T., & Skornia, M. (2023). Energy Sources of Mobile Robot Power Systems: A Systematic Review and Comparison of Efficiency. *Applied Sciences*, *13*(13), 7547. doi: 10.3390/app13137547 (in English).

3. Qin, H., Shao, S., Wang, T., Yu, X., Jiang, Y., & Cao, Z. (2023). Review of autonomous path planning algorithms for mobile robots. *Drones*, *7*(3), 211. doi: 10.3390/drones7030211 (in English).

4. Bruzzone, L., Nodehi, S. E., & Fanghella, P. (2022). Tracked locomotion systems for ground mobile robots: A review. *Machines*, *10*(8), 648. doi: 10.3390/machines10080648 (in English).

5. Seo, T., Ryu, S., Won, J. H., Kim, Y., & Kim, H. S. (2023). Stair-Climbing Robots: A Review on Mechanism, Sensing, and Performance Evaluation. *IEEE Access*, *11*, 60539–60561. doi: 10.1109/ACCESS.2023.3286871 (in English).

6. SWORDS Combat Robot Opens Possibilities; Perhaps Not the way You'd Expect. Retrieved from: https://www.sarna.net/news/swords-combat-robot-opens-possibilities-perhaps-not-the-way-youd-expect/ (in English).

7. Remotec ANDROS Mark V-A1 Robot. Retrieved from: https://www.azorobotics.com/equipment-details.aspx?EquipID=412 (in English).

8. Centaur Unmanned Ground Vehicle. Retrieved from: https://www.army-technology.com/projects/centaur-unmanned-ground-vehicle/ (in English).

9. EOD-Roboter tEODor EVO. Retrieved from: https://esut.de/2019/03/meldungen/land/11637/eod-roboter-teodor-evo/ (in English).

10. Media Gallery: TELEMAX™ EVO. Retrieved from: https://www.avinc.com/media_center/assets/unmanned-ground-vehicles/telemax-evo (in English).

11. Clearpath Grizzly and Husky More Flexible Than Ever. Retrieved from: https://blog.robotiq.com/clearpath-grizzly-and-husky-more-felxible-than-ever (in English).

12. Korendiy, V. (2021). Generalized design diagram and mathematical model of suspension system of vibration-driven robot. *Ukrainian Journal of Mechanical Engineering and Materials Science*, *7*(3–4), 1–10. doi: 10.23939/ujmems2021.03-04.001 (in English).

13. Korendiy, V., Kachur, O., Predko, R., Kotsiumbas, O., Brytkovskyi, V., & Ostashuk, M. (2023). Development and investigation of the vibration-driven in-pipe robot. *Vibroengineering Procedia*, *50*, 1–7. doi: 10.21595/vp.2023.23513 (in English).

14. Wang, C., Lv, W., Li, X., & Mei, M. (2018). Terrain Adaptive Estimation of Instantaneous Centres of Rotation for Tracked Robots. *Complexity*, *2018*, 1–10. doi: 10.1155/2018/4816712 (in English).

15. BaniHani, S., Hayajneh, M. R. M., Al-Jarrah, A., & Mutawe, S. (2021). New control approaches for trajectory tracking and motion planning of unmanned tracked robot. *Advances in Electrical and Electronic Engineering*, *19*(1), 42–56. doi: 10.15598/aeee.v19i1.4006 (in English).

16. Ahluwalia, V., Arents, J., Oraby, A., & Greitans, M. (2022). Construction and benchmark of an autonomous tracked mobile robot system. *Robotic Systems and Applications*, *2*(1), 15–28. doi: 10.21595/rsa.2022.22336 (in English).

17. Zhao, J., Zhang, Z., Liu, S., Tao, Y., & Liu, Y. (2022). Design and research of an articulated tracked firefighting robot. *Sensors*, *22*(14), 5086. doi: 10.3390/s22145086 (in English).

18. Wang, C., Wang, S., Ma, H., Zhang, H., Xue, X., Tian, H., & Zhang, L. (2022). Research on the Obstacle-Avoidance Steering Control Strategy of Tracked Inspection Robots. *Applied Sciences*, *12*(20), 10526. doi: 10.3390/app122010526 (in English).

19. Bang, H.-S., Lee, C.-J., Park, M.-H., Cho, J.-H., & Kim, Y.-T. (2022). Outdoor Navigation System of Caterpillar Mobile Robot Based on Multiple Sensors. *Journal of Korean Institute of Intelligent Systems*, *32*(2), 93–100. doi: 10.5391/JKIIS.2022.32.2.93 (in English).

20. Pandey, A., Singh, S., Kumar, P., Pothal, L. K., & Mohanty, R. L. (2022). Design and Analysis of All-Terrain Differential-Driven Caterpillar-Wheeled Based Unmanned Fire Extinguisher Robot. *Journal of Applied Research and Technology*, *20*(5), 529–535. doi: 10.22201/icat.24486736e.2022.20.5.1389 (in English).

21. Li, H., Cui, J., Ma, Y., Tan, J., Cao, X., Yin, C., & Jiang, Z. (2023). Design and Implementation of Autonomous Navigation System Based on Tracked Mobile Robot. *Communications in Computer and Information Science*. *1787*, 329–350. doi: 10.1007/978-981-99-0617-8_23 (in English).

22. Zhao, J., Zhang, J., Liu, H., Wang, J., & Chen, Z. (2023). Path planning for a tracked robot traversing uneven terrains based on tip-over stability. *Asian Journal of Control*, *25*(5), 3569–3583. doi: 10.1002/asjc.3048 (in English).

23. Shafaei, S. M., & Mousazadeh, H. (2023). Experimental comparison of locomotion system performance of ground mobile robots in agricultural drawbar works. *Smart Agricultural Technology*, *3*, 100131. doi: 10.1016/j.atech.2022.100131 (in English).

24. Petrişor, S. M., Simion, M., Bârsan, G., & Hancu, O. (2023). Humanitarian Demining Serial-Tracked Robot: Design and Dynamic Modeling. Machines, 11(5), 548. doi: 10.3390/machines11050548 (in English).

25. Ugenti, A., Galati, R., Mantriota, G., & Reina, G. (2023). Analysis of an all-terrain tracked robot with innovative suspension system. *Mechanism and Machine Theory*, *182*, 105237. doi: 10.1016/j.mechmachtheory.2023.105237 (in English).

Received 14.09.2023; Accepted in revised form 07.11.2023.

АНАЛІЗ КІНЕМАТИЧНИХ ХАРАКТЕРИСТИК МОБІЛЬНОЇ ГУСЕНИЧНОЇ ПЛАТФОРМИ З МАНІПУЛЯТОРОМ ТИПУ SCARA

Анотація. *Автоматизація і роботизація різноманітних виробничо-технологічних процесів у багатьох галузях промисловості є однією із провідних тенденцій розвитку сучасного суспільства. Чималого поширення останнім часом набули промислові роботи, без яких практично неможливо уявити будь-яке новітнє виробництво у галузях машинобудування, приладобудування, фармацевтики, легкої, харчової, переробної, хімічної промисловостей тощо. Також за останні кілька десятиліть сформувався ще один напрям робототехніки – автономні мобільні роботи, який поєднав дослідження у сферах механіки, електроніки та комп'ютерних технологій, зокрема штучного інтелекту.*

Серед найпоширеніших сфер використання автономних мобільних роботів варто відзначити виконання різноманітних технологічних операцій у місцях, небезпечних для життя людей (радіаційно, біологічно чи хімічно забруднених) або непридатних для життя (космос, морські глибини, кратери вулканів тощо). Також мобільні роботи добре зарекомендували себе під час виконання рятувальних операцій у випадках катаклізмів і стихійних лих, антитерористичних операцій, військових дій, розмінування території тощо.

Враховуючи актуальність питання розвитку мобільної робототехніки, у статті запропоновано нову конструкцію автономного роботизованого комплексу, побудованого на базі гусеничного шасі та оснащеного маніпулятором типу SCARA. Основним завданням пропонованого робота є виконання різноманітних технологічних операцій у місцях, де перебування людини є небезпечним або неможливим, зокрема виконання завдань розмінування територій. Під час досліджень детально проаналізовано кінематику маніпулятора з метою встановлення його робочої зони та експериментально протестовано кінематичні параметри гусеничного шасі під час його руху по пересіченій місцевості. Отримані результати можуть бути використані для подальшого удосконалення конструкції й систем керування робота і маніпулятора та визначення конкретних технологічних завдань, які покладатимуться на цю роботизовану платформу.

Ключові слова: *мобільний робот; роботизований комплекс; гусеничне шасі; розміновування територій; кінематика маніпулятора; робоча зона маніпулятора; рух по пересіченій місцевості.*